DOUBLE LAYERED COMPRESSIBLE MASKS

ND Fowkes *and DP Mason†

Industry Representative

Alex Welte[1]

Study Group Participant

T Myers, N Hale, I Griffiths, M Khalique, N Modhien, H. Zha, E. Mubai, K Born, T Magodi, H. Bhana, F Rakotoniaina, P Chiwira

Abstract

Double-masking may be used to reduce the transmission of a virus. If additionally the masks are compressible, with different permeabilities and behaviour under compression, then it may be possible to design a mask that allows for easy breathing under normal breathing conditions but is relatively impermeable under coughing or sneezing conditions. Such a mask could be both comfortable to wear and effective. We obtain analytical solutions for the steady state flow-through behaviour of such a double mask under flow-out conditions. The results show that the reduction in permeability required to produce a relatively impermeable mask under high flux expulsion (sneezing) conditions could be achieved using either a single filter compressible mask or two filters with different poroelastic parameters. The parameters can be more easily adjusted using a double mask. For both single and double mask cases there is an abrupt cut off, whereby through-flux levels reduce from a maximum value to zero as pressure drop levels increase beyond a critical value. Additionally in the double mask case there exists a second steady state solution for particular parameter ranges. This second solution is unlikely to occur under normal circumstances.

*Department of Mathematics and Statistics, University of Western Australia, Crawley, Western Australia, Australia. *email: Neville.Fowkes@uwa.edu.au*

†University of the Witwatersrand, Johannesburg, South Africa, *email: David.Mason@wits.ac.za.*

[1]South African Centre for Epidemiological Research and Analysis, University of Stellenbrosch, Stellenbrosch, South Africa email: *alexwelte@gmail.com*

1 Introduction

There is considerable interest in the use of masks to reduce the spread of Covid-19. In many countries the wearing of a mask is compulsory in public places. Most of the masks in use are 'one filter layer' masks[2]. Dr Fauci, who is the Director of the United States National Institute of Allergy and Infectious diseases, recently advised: "If you have a physical covering with one layer, you put another layer on, it just makes common sense that it likely would be more effective. That is the reason why you see people either double masking or doing a version of an N-95." The MISG in South Africa was asked to contribute to the understanding of the effects of masks on the spread of infectious respiratory droplets as in Covid-19. A subgroup of the Study Group investigated the double mask which could consist of either a mask made of two filter layers with different material properties or two masks in perfect contact with no air gap between the masks. The results obtained by the subgroup is the subject of this article.

Many filters in use can be described as being rigid in the sense that the permeability (and porosity) of such filters remains constant irrespective of the applied pressure drop and accompanying flow through them. By virtue of the difference in porosity between the two layers making up a double mask there can be improved performance, because the two layers can filter out different size particles. Typically the filter/mask closer to the face could be used to capture larger particles, with smaller particles being captured in the outer filter/mask. However filters may be compressible [2],[1] in the sense that the permeability (and porosity) changes with applied pressure and this affects the flow-through as well as particle capture. Such compressibility effects may be used to advantage when designing a double mask. The subgroup considered two compressible masks in which the permeability depends linearly on the deformation gradient of the mask. This article will focus on the fluid flow through the mask/s. A later article will address the associated porosity/particle capture aspects of the problem.

The structure of the paper is as follows. A brief review of poroelasticity is presented in Section 2. In Section 3 the mathematical model of the double compressible mask is formulated. The double compressible mask problem is solved analytically in Section 4. In Section 5 the permeability of each mask and the pressure difference across the double mask are obtained. In Section 6 suitable scales for the fluid flux, permeability and pressure are introduced, and the number of dimensionless parameters is further reduced to highlight the possible outcomes. In Section 7 results are presented in the simpler '(incompressible) rigid masks' case. The results in the general case are fully analysed with the aid of graphs in Section 8. Finally conclusions are drawn in Section 9.

[2]Sometimes masks have a thin outer moisture repelling layer and a thin inner moisture absorbing layer which are not acting as particle filters and do not restrict flow.

2 Poroelasticity

The mask will be modelled as a solid in the form of an elastic matrix containing small pores. The pores are connected which allows the flow of viscous fluid through the mask. Poroelasticity can therefore be applied to model the mask. We first give a brief review of poroelesticity of an isotropic medium, [3].

The net stress tensor of the medium is the sum of an elastic stress tensor of the matrix and a stress tensor describing the pore fluid. The medium is isotropic and homogeneous. The elastic contribution to the stress tensor in Cartesian coordinates $(x_1,\, x_2,\, x_3)$ is

$$\tau(\mathrm{e})_{ik} = \lambda_{\mathit{eff}} \big(\boldsymbol{\nabla}\cdot\mathbf{u}\big)\, \delta_{ik} + 2\,\mu_{\mathit{eff}}\, E_{ik} \tag{2.1}$$

where $\mathbf{u}$ is the displacement vector, $\boldsymbol{\nabla}$ is the del vector operator and E_{ik} is the strain tensor,

$$E_{ik} = \frac{1}{2}\left(\frac{\partial u_i}{\partial x_k} + \frac{\partial u_k}{\partial x_i}\right) . \tag{2.2}$$

The effective Lamé constants, λ_{eff} and μ_{eff}, are different from the Lamé constants of the material of the matrix. It is assumed that the stress in the fluid averages, on a length scale of many pore sizes, to an isotropic pore fluid pressure P with stress tensor

$$\tau(f)_{ik} = -P\,\delta_{ik} \; . \tag{2.3}$$

The net stress tensor of the porous elastic medium is therefore

$$\tau_{ik} = \tau(\mathrm{e})_{ik} + \tau(f)_{ik} = \big(-P + \lambda_{\mathit{eff}}\,\boldsymbol{\nabla}\cdot\mathbf{u}\big)\,\delta_{ik} + \mu_{\mathit{eff}}\left(\frac{\partial u_i}{\partial x_k} + \frac{\partial u_k}{\partial x_i}\right) . \tag{2.4}$$

The inertia and body force due to gravity will be neglected. The net stress tensor therefore satisfies the equations of static equilibrium

$$\frac{\partial}{\partial x_k}\,\tau_{ki} = 0\,, \qquad i = 1,2,3\;. \tag{2.5}$$

Substituting (2.4) into (2.5) leads to the Navier displacement equation for static equilibrium

$$\mu_{\mathit{eff}}\nabla^2\mathbf{u} + (\lambda_{\mathit{eff}} + \mu_{\mathit{eff}})\,\boldsymbol{\nabla}(\boldsymbol{\nabla}\cdot\mathbf{u}) = \boldsymbol{\nabla}P\;. \tag{2.6}$$

The fluid flux $\mathbf{q}$ is the volume flow rate per unit surface area through the porous medium. It satisfies Darcy's law

$$\mathbf{q} = -\frac{K}{\eta}\,\boldsymbol{\nabla}P \tag{2.7}$$

where η is the viscosity of the fluid and K is the permeability of the medium. The velocity of the solid matrix is neglected in (2.7)

The remaining condition to impose is conservation of mass. We neglect the compressibility of the fluid and solid matrix and make the approximation of a steady state. Then [3]

$$\boldsymbol{\nabla}\cdot\mathbf{q} = 0\;. \tag{2.8}$$

The matrix as a whole, however, is compressible.

We will assume that λ_{eff}, μ_{eff} and η are constant but the mask is compressible and the permeability will depend on the displacement gradient.

The permeability is closely related to the porosity, ϕ, of the medium. An example of the relationship is the Kozeney-Carman equation

$$K = \frac{K_0\phi^3}{(1-\phi)^2} \;, \qquad \frac{\mathrm{d}K}{\mathrm{d}\phi} = \frac{K_0(3-\phi)\phi^2}{(1-\phi)^3} \;, \qquad 0 < \phi < 1 \;, \tag{2.9}$$

according to which the permeability is an increasing function of ϕ. We will not impose a specific constitutive equation between the permeability and the porosity, since we will not be addressing particle capture issues in this article. Instead we will work directly with the permeability in the two masks.

3 Mathematical model for a two layer compressible mask

A two layer mask could consist either of two masks in perfect contact with no air gap between them or a mask made of two layers of different material. A model of a two layer compressible mask is illustrated in Figure 1. It is assumed that the mask can be represented by a one-dimensional model. Mask 1 or layer 1 extends from $0 \le x \le L_1$ while Mask 2 or layer 2 is of width L_2 and extends from $L_1 \le x \le L$ where $L = L_1 + L_2$. There is an effective porous grid attached to Mask 1 at $x = 0$. Fluid can flow through the porous grid without resistance and it is held in position by the mask belt which extends round the head of the wearer of the mask. The fluid flows through the two masks due to an imposed pressure difference, $P_{\text{in}} - P_{\text{out}}$, where P_{in} is the pressure at the mouth of the wearer, $x = L$ and P_{out} is the pressure at the porous grid, $x = 0$. Since the model is assumed to be one-dimensional all quantities depend only on x. The quantities of Mask 1 are denoted by suffix 1 and Mask 2 by suffix 2. Thus

$$\mathbf{u}_n = \big(u_n(x), 0, 0\big) \;, \qquad P_n = P_n(x) \;, \qquad n = 1, 2 \;. \tag{3.1}$$

We take the fluid flux to be positive in the negative x-direction so that the fluid flux from the mouth and nose into the mask is positive. Hence

$$\mathbf{q}_n = \big(-q_n(x), 0, 0\big), \qquad n = 1, 2 \;, \tag{3.2}$$

where $q_n(x) \ge 0$. In order to simplify the notation, λ_{eff} and μ_{eff} will be denoted by λ and μ. Since the same fluid flows through both masks the fluid viscosity is denoted simply by η.

Only the x-components of the equations of poroelasticity in Section 2 are not identically zero. The x-component of the Navier displacement equation (2.6) in each layer is

$$\Big(\lambda_n + 2\mu_n\Big)\frac{\mathrm{d}^2 u_n}{\mathrm{d}x^2} = \frac{\mathrm{d}P_n}{\mathrm{d}x} \;, \qquad n = 1, 2 \;. \tag{3.3}$$

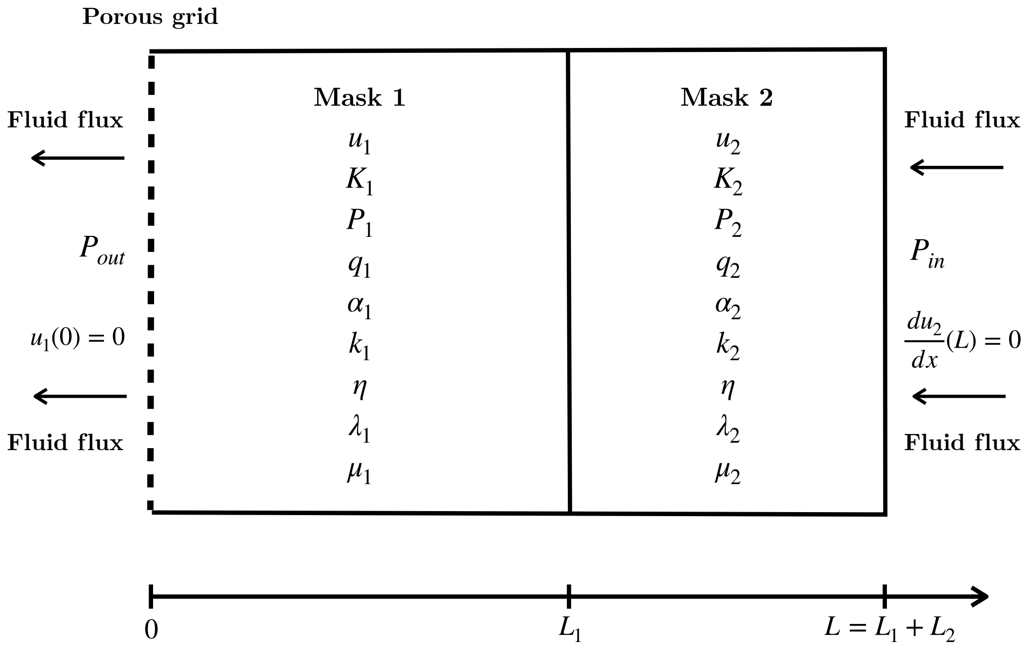

Figure 1: One-dimensional model of a two layer compressible mask.

The x-component of Darcy's law, (2.7), is

$$q_n(x) = \frac{K_n}{\eta}\,\frac{\mathrm{d}P_n}{\mathrm{d}x}\,, \qquad n = 1, 2\,. \tag{3.4}$$

For a compressible mask the permeability of the material is assumed to depend on the displacement gradient $\frac{\mathrm{d}u}{\mathrm{d}x}$. We use the linear constitutive equation [1, 2]

$$K_n = k_n + \alpha_n^*\,\frac{\mathrm{d}u_n}{\mathrm{d}x}\,, \qquad n = 1, 2\,, \tag{3.5}$$

where k_n is the permeability of the medium in its undeformed state and is a positive constant. We assume also that the constant $\alpha^* > 0$. We write

$$K_n = k_n\left(1 + \alpha_n\,\frac{\mathrm{d}u_n}{\mathrm{d}x}\right) \tag{3.6}$$

where $\alpha_n = \alpha_n^*/k_n$. The constant α_n is dimensionless and is a suitable small perturbation parameter to determine compressibility effects since for the rigid mask, $\alpha_n = 0$. Equation (3.4) becomes

$$q_n(x) = \frac{k_n}{\eta}\left(1 + \alpha_n\,\frac{\mathrm{d}u_n}{\mathrm{d}x}\right)\,\frac{\mathrm{d}P_n}{\mathrm{d}x}\,. \tag{3.7}$$

The conservation of mass equation (2.8) reduces to

$$\frac{\mathrm{d}q_n}{\mathrm{d}x} = 0\,, \qquad n = 1, 2\,. \tag{3.8}$$

Consider next the boundary conditions. Mask 1 is attached to a porous grid at $x = 0$. The displacement at $x = 0$ must therefore be zero:

$$u_1(0) = 0\ . \tag{3.9}$$

At $x = L$, the end is not compressed and therefore is free of applied stress. Thus from (2.1)

$$\tau^{(2)}(\mathrm{e})_{xx} = \left(\lambda_2 + 2\mu_2\right) \frac{\mathrm{d}u_2}{\mathrm{d}x}\ (L) = 0\ . \tag{3.10}$$

The pressure at $x = 0$ and $x = L$ is P_{out} and P_{in} which are constants. Hence

$$P_1(0) = P_{\mathrm{out}}\ , \qquad P_2(L) = P_{\mathrm{in}}\ . \tag{3.11}$$

The pressure P_{in} is prescribed but we will see that the fluid flux and the pressure P_{out} cannot both be prescribed.

Finally there are matching conditions at the interface between the masks at $x = L_1$. We assume that the two masks are in perfect contact and therefore at $x = L_1$ the displacement is continuous,

$$u_1(L_1) = u_2\ (L_1) \tag{3.12}$$

and the fluid flux is continuous

$$q_1(L_1) = q_2\ (L_1)\ . \tag{3.13}$$

The normal elastic stress is also continuous at $x = L_1$,

$$\tau^{(1)}(\mathrm{e})_{xx}\ (L_1) = \tau^{(2)}(\mathrm{e})_{xx}\ (L_1)\ , \tag{3.14}$$

and from (2.1) this gives the matching condition

$$\left(\lambda_1 + 2\mu_1\right) \frac{\mathrm{d}u_1}{\mathrm{d}x}\ (L_1) = \left(\lambda_2 + 2\mu_2\right) \frac{\mathrm{d}u_2}{\mathrm{d}x}\ (L_1)\ . \tag{3.15}$$

Since the stress in the fluid is continuous at $x = L_1$ the pore fluid pressure is continuous. Hence

$$P_1(L_1) = P_2(L_1)\ . \tag{3.16}$$

We will be interested in the flow for which $P_{\mathrm{in}} > P_{\mathrm{out}}$. The mask is then under compression since the porous grid is fixed at $x = 0$. The fluid flows in the negative x-direction and the x-component of the fluid flux in (3.2), $q_n(x)$, is positive. The model also applies for $P_{\mathrm{out}} > P_{\mathrm{in}}$.

The problem is to solve the six equations (3.3), (3.7) and (3.8) for the six quantities $u_n(x)$, $P_n(x)$ and $q_n(x)$ where $n = 1$ and 2, subject to the boundary conditions (3.9), (3.10) and (3.11) and the matching conditions (3.12),(3.13),(3.15) and (3.16).

We do not make the equations dimensionless because we find that the solution can be expressed in terms of the ratios of α, k and $\lambda + 2\mu$ in the two layers.

4 Solution for the two layer compressible mask

From (3.8)

$$q_n(x) = q_{n0} \ , \qquad n = 1, 2 \tag{4.1}$$

where q_{n0} is a constant. But from the matching condition (3.13),

$$q_{10} = q_{20} = q_0 \tag{4.2}$$

where q_0 is a constant.

Equation (3.7) becomes

$$\frac{\mathrm{d}P_n}{\mathrm{d}x} = \frac{q_0 \eta}{k_n} \left[1 + \alpha_n \, \frac{\mathrm{d}u_n}{\mathrm{d}x} \right]^{-1} \tag{4.3}$$

and by inserting (4.3) in (3.3) we obtain for u_n the second order differential equation

$$\frac{\mathrm{d}^2 u_n}{\mathrm{d}x^2} + \alpha_n \, \frac{\mathrm{d}u_n}{\mathrm{d}x} \, \frac{\mathrm{d}^2 u_n}{\mathrm{d}x^2} = \frac{q_0 \, \eta}{k_n \big(\lambda_n + 2\mu_n \big)} \ . \tag{4.4}$$

Equation (4.4) can be rewritten as

$$\frac{\mathrm{d}^2 u_n}{\mathrm{d}x^2} + \frac{\alpha_n}{2} \, \frac{\mathrm{d}}{\mathrm{d}x} \left(\left(\frac{\mathrm{d}u_n}{\mathrm{d}x} \right)^2 \right) = \frac{q_0 \, \eta}{k_n \big(\lambda_n + 2\mu_n \big)} \tag{4.5}$$

and by integrating with respect to x we obtain

$$\frac{\alpha_n}{2} \left(\frac{\mathrm{d}u_n}{\mathrm{d}x} \right)^2 + \frac{\mathrm{d}u_n}{\mathrm{d}x} - \left(A_n + \frac{q_0 \, \eta}{k_n \big(\lambda_n + 2\mu_n \big)} \, x \right) = 0 \ , \tag{4.6}$$

where A_n is a constant. Equation (4.6) is a quadratic equation for $\frac{\mathrm{d}u_n}{\mathrm{d}x}$. Hence

$$\frac{\mathrm{d}u_n}{\mathrm{d}x} = -\frac{1}{\alpha_n} \pm \frac{1}{\alpha_n} \left[1 + 2\alpha_n \left(A_n + \frac{q_0 \, \eta}{k_n \big(\lambda_n + 2\mu_n \big)} \, x \right) \right]^{\frac{1}{2}} \ . \tag{4.7}$$

In order to decide which sign to take in (4.7) we expand (4.7) for small values of α_n and compare with the corresponding result for a rigid two layer mask. Now

$$\frac{\mathrm{d}u_n}{\mathrm{d}x} = -\frac{1}{\alpha_n} \pm \frac{1}{\alpha_n} \pm \left(A_n + \frac{q_0 \, \eta}{k_n \big(\lambda_n + 2\mu_n \big)} \, x \right) + \mathrm{O}\,(\alpha) \qquad \text{as } \alpha \to 0 \ . \tag{4.8}$$

But for a rigid mask, $\alpha_n = 0$ and solving in the same way as for a compressible mask we find that, instead of (4.8),

$$\frac{\mathrm{d}u_n}{\mathrm{d}x} = A_{0n} + \frac{q_0 \, \eta}{k_n \big(\lambda_n + 2\mu_n \big)} \, x \ , \tag{4.9}$$

where A_{0n} is a constant. By letting $\alpha_n \to 0$ in (4.8) we see that the + sign must be taken in (4.7). The constant A_n could depend on α_n but in such a way that it tends to the finite constant A_{0n} as $\alpha_n \to 0$. Equation (4.7) becomes

$$\frac{\mathrm{d}u_n}{\mathrm{d}x} = -\frac{1}{\alpha_n} + \frac{1}{\alpha_n}\left[1 + 2\alpha_n\left(A_n + \frac{q_0\,\eta}{k_n\big(\lambda_n + 2\mu_n\big)}\,x\right)\right]^{\frac{1}{2}} \tag{4.10}$$

and by integrating again we obtain for the displacement

$$u_n(x) = -\frac{x}{\alpha_n} + \frac{k_n(\lambda_n + 2\mu_n)}{3\,\alpha_n^2\,q_0\,\eta}\left[1 + 2\alpha_n\left(A_n + \frac{q_0\,\eta}{k_n\big(\lambda_n + 2\mu_n\big)}\,x\right)\right]^{\frac{3}{2}} + B_n \tag{4.11}$$

where B_n is a constant.

The pressure in the fluid, $P_n(x)$, is obtained by substituting (4.10) into (4.3). This gives

$$\frac{\mathrm{d}P_n}{\mathrm{d}x} = \frac{q_0\,\eta}{k_n}\left[1 + 2\alpha_n\left(A_n + \frac{q_0\,\eta}{k_n\big(\lambda_n + 2\mu_n\big)}\,x\right)\right]^{-\frac{1}{2}} \tag{4.12}$$

and by integrating with respect to x we obtain

$$P_n(x) = \frac{\big(\lambda_n + 2\mu_n\big)}{\alpha_n}\left[1 + 2\alpha_n\left(A_n + \frac{q_0\eta}{k_n\big(\lambda_n + 2\mu_n\big)}\,x\right)\right]^{\frac{1}{2}} + C_n \tag{4.13}$$

where C_n is a constant.

We now apply the boundary conditions. Imposing the boundary conditions (3.9) on (4.11), (3.10) on (4.10) and the first condition in (3.11) on (4.13) gives

$$\frac{k_1\big(\lambda_1 + 2\mu_1\big)}{3\alpha_1^2\,q_0\,\eta}\,\big(1 + 2\alpha_1\,A_1\big)^{\frac{1}{2}} + B_1 = 0\,, \tag{4.14}$$

$$A_2 = -\frac{q_0\,\eta\,L}{k_2\big(\lambda_2 + 2\mu_2\big)}\,, \tag{4.15}$$

$$\frac{\big(\lambda_1 + 2\mu_1\big)}{\alpha_1}\,\big(1 + 2\alpha_1\,A_1\big)^{\frac{1}{2}} + C_1 = P_{\mathrm{out}}\,. \tag{4.16}$$

Imposing the second pressure boundary condition in (3.11) on (4.13) and using (4.15) gives

$$C_2 = P_{\mathrm{in}} - \frac{\big(\lambda_2 + 2\mu_2\big)}{\alpha_2}\,. \tag{4.17}$$

It remains to impose the matching conditions at the interface $x = L_1$. By using (4.11) for $u_n(x)$ and replacing A_2 in terms of q_0 by (4.15), the matching condition

(3.12) becomes

$$-\frac{L_1}{\alpha_1}+\frac{k_1(\lambda_1+2\mu_1)}{3\alpha_1^2\,q_0\,\eta}\left[1+2\alpha_1\left(A_1+\frac{q_0\,\eta\,L_1}{k_1(\lambda_1+2\mu_1)}\right)\right]^{\frac{3}{2}}+B_1$$

$$=-\frac{L_1}{\alpha_2}+\frac{k_2(\lambda_2+2\mu_2)}{3\alpha_2^2\,q_0\,\eta}\left[1-\frac{2\alpha_2\,q_0\,\eta(L-L_1)}{k_2(\lambda_2+2\mu_2)}\right]^{\frac{3}{2}}+B_2\ . \tag{4.18}$$

By using (4.10) and eliminating A_2 with (4.15) the matching condition (3.15) becomes

$$(\lambda_1+2\mu_1)\left[-\frac{1}{\alpha_1}+\frac{1}{\alpha_1}\left[1+2\alpha_1\left(A_1+\frac{q_0\,\eta\,L_1}{k_1(\lambda_1+2\mu_1)}\right)\right]^{\frac{1}{2}}\right]$$

$$=(\lambda_2+2\mu_2)\left[-\frac{1}{\alpha_2}+\frac{1}{\alpha_2}\left[1-\frac{2\alpha_2\,q_0\,\eta(L-L_1)}{k_2(\lambda_2+2\mu_2)}\right]^{\frac{1}{2}}\right]\ . \tag{4.19}$$

The remaining matching condition (3.16) becomes, using (4.13) for $P_n(x)$, (4.15) for A_2 and (4.17) for C_2,

$$\frac{\lambda_1+2\mu_1)}{\alpha_1}\left[1+2\alpha_1\left(A_1+\frac{q_0\,\eta_1\,L_1}{k_1(\lambda_1+2\mu_1)}\right)\right]^{\frac{1}{2}}+C_1$$

$$=\frac{(\lambda_2+2\mu_2)}{\alpha_2}\left[1-\frac{2\alpha_2\,q_0\,\eta(L-L_1)}{k_2(\lambda_2+2\mu_2)}\right]^{\frac{1}{2}}-\frac{(\lambda_2+2\mu_2)}{\alpha_2}+P_{\rm in}\ . \tag{4.20}$$

There are eight quantities, A_1, B_1, C_1, A_2, B_2, C_2, q_0 and $P_{\rm out}$ and there are seven equations, (4.14) to (4.20). Since $P_{\rm in}$ is prescribed the constant C_2 is given by (4.17). The constant A_2 is determined in terms of q_0 from (4.15) while A_1 is determined in terms of q_0 from the matching condition (4.19). With A_1 determined in terms of q_0, B_1 and C_1 are obtained in terms of q_0 from (4.14) and (4.20) while B_2 is now obtained in terms of q_0 from (4.18). Since A_1 and C_1 can be expressed in terms of q_0, the remaining boundary condition (4.16) is a relation between q_0 and $P_{\rm out}$. The fluid flux q_0 and the exit pressure $P_{\rm out}$ cannot both be prescribed. Either q_0 or $P_{\rm out}$ is prescribed. The quantity not prescribed is then determined from (4.16).

Where possible the constants are expressed in terms of the ratio of the parameters in the two masks. The following results are obtained for the constants:

$$
\begin{aligned}
A_1 &= -\frac{q_o\,\eta\,L_1}{k_1\big(\lambda_1+2\mu_1\big)} - \frac{1}{2\alpha_1} \\
&+ \frac{1}{2\alpha_1}\left[1-\frac{\alpha_1}{\alpha_2}\left(\frac{\lambda_2+2\mu_2}{\lambda_1+2\mu_1}\right)\left\{1-\left(1-\frac{2\alpha_2\,q_0\,\eta\,L_2}{k_2\big(\lambda_2+2\mu_2\big)}\right)^{\frac{1}{2}}\right\}\right]^2 \qquad (4.21)
\end{aligned}
$$

$$
C_1 = P_{\rm in} - \frac{\big(\lambda_1+2\mu_1\big)}{\alpha_1}\,, \qquad (4.22)
$$

$$
B_1 = -\frac{k_1\big(\lambda_1+2\mu_1\big)}{3\alpha_1^2\,q_0\,\eta}\,\big(1+2\alpha_1\,A_1\big)^{\frac{3}{2}}\,, \qquad (4.23)
$$

$$
\begin{aligned}
B_2 &= L_1\left(\frac{1}{\alpha_2}-\frac{1}{\alpha_1}\right) \\
&+ \frac{k_1\big(\lambda_1+2\mu_1\big)}{3\alpha_1^2\,q_0\,\eta}\left[\left(1+2\alpha_1\,A_1+\frac{2\alpha_1\,q_0\,\eta\,L_1}{k_1\big(\lambda_1+2\mu_1\big)}\right)^{\frac{3}{2}} - \Big(1+2\alpha_1\,A_1\Big)^{\frac{3}{2}}\right] \\
&- \frac{k_2\big(\lambda_2+2\mu_2\big)}{3\alpha_2^2\,q_0\,\eta}\left[1-\frac{2\alpha_2\,q_0\,\eta\,\big(L-L_1\big)}{k_2\big(\lambda_2+2\mu_2\big)}\right]^{\frac{3}{2}}\,. \qquad (4.24)
\end{aligned}
$$

We will be mainly interested in the permeabilities, K_1 and K_2 which depend on A_1 and A_2 and in the pressure difference, $P_{\rm in}$-$P_{\rm out}$, which depends on A_1 and C_1. The displacements, u_1 and u_2, depend on B_1 and B_2 which depend on A_1 given by (4.21). Equation (4.16) which is the relation between q_0 and $P_{\rm out}$ becomes

$$
P_{\rm in} - P_{\rm out} = \frac{\big(\lambda_1+2\mu_1\big)}{\alpha_1}\left[1-\Big(1+2\alpha_1\,A_1\Big)^{\frac{1}{2}}\right] \qquad (4.25)
$$

where

$$
\begin{aligned}
1\;+\;2\alpha_1\,A_1 &= -\frac{2\alpha_1\,q_0\,\eta\,L_1}{k_1\big(\lambda_1+2\mu_1\big)} \\
&+ \left[1-\frac{\alpha_1}{\alpha_2}\,\frac{\big(\lambda_2+2\mu_2\big)}{\big(\lambda_1+2\mu_1\big)}+\frac{\alpha_1}{\alpha_2}\,\frac{\big(\lambda_2+2\mu_2\big)}{\big(\lambda_1+2\mu_1\big)}\left(1-\frac{2\alpha_2\,q_0\,\eta\,L_2}{k_2\big(\lambda_2+2\mu_2\big)}\right)^{\frac{1}{2}}\right]^2\,. \qquad (4.26)
\end{aligned}
$$

5 Physical quantities

The permeability of each mask is obtained from (3.6) and (4.10):

$$K_n(x) = k_n \left[1 + 2\alpha_n \left(A_n + \frac{q_0\,\eta}{k_n\big(\lambda_n + 2\mu_n\big)}\; x \right) \right]^{\frac{1}{2}} , \quad n = 1, 2\,. \tag{5.1}$$

By using (4.26) for A_1 and (4.15) for A_2 we find that

$$K_1(x) = k_1 \left[-\frac{2\alpha_1\, q_0\, \eta}{k_1\big(\lambda_1 + 2\mu_1\big)}\; (L_1 - x) \right.$$

$$\left. + \left(1 - \frac{\alpha_1}{\alpha_2}\, \frac{\big(\lambda_2 + 2\mu_2\big)}{\big(\lambda_1 + 2\mu_1\big)} + \frac{\alpha_1}{\alpha_2}\, \frac{\big(\lambda_2 + 2\mu_2\big)}{\big(\lambda_1 + 2\mu_1\big)} \left(1 - \frac{2\alpha_2\, q_0\, \eta\, L_2}{k_2\big(\lambda_2 + 2\mu_2\big)} \right)^{\frac{1}{2}} \right)^2 \right]^{\frac{1}{2}} \tag{5.2}$$

for $0 \le x \le L_1$ and

$$K_2(x) = k_2 \left[1 - \frac{2\alpha_2\, q_0\, \eta}{k_2\big(\lambda_2 + 2\mu_2\big)}\; (L - x) \right]^{\frac{1}{2}} \tag{5.3}$$

for $L_1 \le x \le L$.

The fluid pressure is given by (4.13) for $n = 1$ and 2. By using (4.26), (4.15), (4.22) and (4.17) for A_1, A_2, C_1 and C_2 it can be verified that

$$P_1(x) = P_{\rm in} - \frac{\big(\lambda_1 + 2\mu_1\big)}{\alpha_1} \left[1 - \left(-\frac{2\alpha_1\, q_0\, \eta}{k_1\big(\lambda_1 + 2\mu_1\big)}\; \big(L_1 - x\big) + \right.\right.$$

$$\left.\left. \left[1 - \frac{\alpha_1}{\alpha_2}\, \frac{\big(\lambda_2 + 2\mu_2\big)}{\big(\lambda_1 + 2\mu_1\big)} + \frac{\alpha_1}{\alpha_2}\, \frac{\big(\lambda_2 + 2\mu_2\big)}{\big(\lambda_1 + 2\mu_1\big)} \left(1 - \frac{2\alpha_2\, q_0\, \eta\, L_2}{k_2\big(\lambda_2 + 2\mu_2\big)} \right)^{\frac{1}{2}} \right]^2 \right)^{\frac{1}{2}} \right] \tag{5.4}$$

for $0 \le x \le L_1$ and

$$P_2(x) = P_{\rm in} - \frac{\big(\lambda_2 + 2\mu_2\big)}{\alpha_2} \left[1 - \left(1 - \frac{2\alpha_2\, q_0\, \eta}{k_2\big(\lambda_2 + 2\mu_2\big)}\; (L - x) \right)^{\frac{1}{2}} \right] \tag{5.5}$$

for $L_1 \le x \le L$.

The difference between the fluid pressure at the entry at Mask 2, $x = L$, and at the exit at Mask 1, $x = 0$, is given by (4.25). By using again (4.26) the following relation between q_0 and $P_{\rm out}$ is obtained:

$$P_{\rm in} - P_{\rm out} = \frac{\big(\lambda_1 + 2\mu_1\big)}{\alpha_1} \left[1 - \left(-\frac{2\alpha_1\, q_0\, \eta\, L_1}{k_1\big(\lambda_1 + 2\mu_1\big)} \right.\right.$$

$$\left.\left. + \left[1 - \frac{\alpha_1}{\alpha_2}\, \frac{\big(\lambda_2 + 2\mu_2\big)}{\big(\lambda_1 + 2\mu_1\big)} + \frac{\alpha_1}{\alpha_2}\, \frac{\big(\lambda_2 + 2\mu_2\big)}{\big(\lambda_1 + 2\mu_1\big)} \left(1 - \frac{2\alpha_2\, q_0\, \eta\, L_2}{k_2\big(\lambda_2 + 2\mu_2\big)} \right)^{\frac{1}{2}} \right]^2 \right)^{\frac{1}{2}} \right] . \tag{5.6}$$

It is readily verified that (5.6) agrees with (5.4) evaluated at $x = 0$.

The displacement components, $u_1(x)$ and $u_2(x)$, are given by (4.11) where B_1 and B_2 are given by (4.23) and (4.24). The constants B_1 and B_2 are expressed in terms of $1 + 2\alpha_1 A_1$ and can be expanded using again (4.26). We will not analyse $u_1(x)$ and $u_2(x)$ since it is sufficient to investigate the properties of the permeability and pressure difference across the double mask in order to understand the working of the double mask.

6 Scaled quantities and parameter reduction

We first introduce scaled physical quantities. On examining the equations for the scaled quantities we see that we can reduce the number of dimensionless parameters.

6.1 Scaled quantities

From (5.3) the permeability $K_2(x)$ is real for values of x in the range $L_1 \le x \le L$ provided

$$q_0 \le q_s \qquad \text{where} \qquad q_s = \frac{k_2\big(\lambda_2 + 2\mu_2\big)}{2\alpha_2\,\eta\,L_2}\,. \tag{6.1}$$

We choose the following scales for the physical variables in both masks:

$$\begin{aligned} &\text{fluid flux scale} = q_s\,, && \text{fluid pressure scale } P_s = \frac{\lambda_1 + 2\mu_1}{\alpha_1}\,,\\ &\text{permeability scale } = k_2\,, && \text{length scale} = L\,. \end{aligned}$$

We emphasise that the scales are not characteristic quantities. They are suitable scales that produce dimensionless variables and give a useful way to present the results. In order to obtain the actual pressure, for example, we would need to multiply the scaled result by P_s.

The scale q_s is the maximum value for the fluid flux in Mask 2, and therefore in the double mask, for given values of α_2, λ_2, μ_2, k_2 and L_2. It depends only on the parameters and width of Mask 2. The pressure scale P_s is a factor in the pressure difference (5.6) across the double mask. The scale P_s for given values of α_1, λ_1 and μ_1 depends only on the parameters in Mask 1. It is used to scale the pressure in both Mask 1 and Mask 2. The permeability scale, k_2, is the permeability of Mask 2 in its undeformed state. The length L is based on the width of the double mask because we are interested, for example, in the pressure difference across the double mask.

We define the following scaled quantities:

$$q_0^* = \frac{q_0}{q_s} , \qquad 0 \le q_0^* \le 1 , \tag{6.2}$$

$$x^* = \frac{x}{L} \quad (0 \le x^* \le 1) , \qquad L_1^* = \frac{L_1}{L} , \qquad L_2^* = \frac{L_2}{L} , \tag{6.3}$$

$$L_1^* + L_2^* = 1 , \tag{6.4}$$

$$K_1^*(x^*) = \frac{K_1(x)}{k_2} , \qquad K_2^*(x^*) = \frac{K_2(x)}{k_2} , \tag{6.5}$$

$$P_1^*(x^*) = \frac{P_1(x)}{P_s} , \quad P_2^*(x^*) = \frac{P_2(x)}{P_s} , \quad \left(P_{\text{in}} - P_{\text{out}}\right)^* = \frac{P_{\text{in}} - P_{\text{out}}}{P_s} . \tag{6.6}$$

From (5.2) and (5.3) the scaled permeabilities in Mask 1 and Mask 2 are,

$$K_1^*(x^*) = \frac{k_1}{k_2} \left[\left(1 - \frac{\alpha_1}{\alpha_2} \frac{\left(\lambda_2 + 2\mu_2\right)}{\left(\lambda_1 + 2\mu_1\right)} + \frac{\alpha_1}{\alpha_2} \frac{\left(\lambda_2 + 2\mu_2\right)}{\left(\lambda_1 + 2\mu_1\right)} \left(1 - q_0^*\right)^{\frac{1}{2}} \right)^2 - \frac{\alpha_1}{\alpha_2} \frac{\left(\lambda_2 + 2\mu_2\right)}{\left(\lambda_1 + 2\mu_1\right)} \frac{k_2}{k_1} q_0^* \frac{\left(L_1^* - x^*\right)}{\left(1 - L_1^*\right)} \right]^{\frac{1}{2}} \tag{6.7}$$

for $0 \le x^* \le L_1^*$ and

$$K_2^*(x^*) = \left[1 - q_0^* \frac{(1 - x*)}{(1 - L_1^*)} \right]^{\frac{1}{2}} \tag{6.8}$$

for $L_1^* \le x^* \le 1$. From (5.6) the scaled pressure difference across the double mask is

$$P_{\text{in}}^* - P_{\text{out}}^* = 1 - \left[\left(1 - \frac{\alpha_1}{\alpha_2} \frac{\left(\lambda_2 + 2\mu_2\right)}{\left(\lambda_1 + 2\mu_1\right)} + \frac{\alpha_1}{\alpha_2} \frac{\left(\lambda_2 + 2\mu_2\right)}{\left(\lambda_1 + 2\mu_1\right)} \left(1 - q_0^*\right)^{\frac{1}{2}} \right)^2 - \frac{\alpha_1}{\alpha_2} \frac{\left(\lambda_2 + 2\mu_2\right)}{\left(\lambda_1 + 2\mu_1\right)} \frac{k_2}{k_1} q_0^* \frac{L_1^*}{\left(1 - L_1^*\right)} \right]^{\frac{1}{2}} . \tag{6.9}$$

Equation (6.9) is a relation between q_0^* and P_{out}. Only one of q_0^* and P_{out}^* can be specified, the other is obtained from (6.9).

The fluid pressure is continuous across the interface $x = L_1$ and it is readily verified from (5.4) and (5.5) that $P_1(x)$ for $0 \le x \le L_1$ and $P_2(x)$ for $L_1 \le x \le L$ are increasing functions of x. The quantity of interest is the pressure difference (5.6) across the double mask. We will therefore not investigate $P_1(x)$ and $P_2(x)$ in each mask separately and therefore do not write $P_1(x)$ and $P_2(x)$ in scaled form.

The results will be fully analysed in Section 8. We give here a few elementary properties of the solutions. From (6.7) and (6.8),

$$\frac{\mathrm{d}K_1^*}{\mathrm{d}x^*} = \frac{1}{2}\,\frac{\alpha_1}{\alpha_2}\,\frac{\left(\lambda_2+2\mu_2\right)}{\left(\lambda_1+2\mu_1\right)}\,\frac{k_1}{k_2}\,\frac{q_0^*}{K_1^*(x^*)\left(1-L_1^*\right)} > 0\ ,\ \ 0 \le x^* \le L_1^*\ , \tag{6.10}$$

$$\frac{\mathrm{d}K_2^*}{\mathrm{d}x^*} = \frac{q_0^*}{2K_2^*(x^*)(1-L_1^*)} > 0\ , \qquad L_1^* \le x^* \le 1\ . \tag{6.11}$$

Hence $K_1^*(x^*)$ and $K_2^*(x^*)$ are increasing functions of x^*. In general the permeabilities $K_1^*(x^*)$ and $K_2^*(x^*)$ will not be equal at the interface $x^* = L_1^*$. It can be verified that

$$K_1^*\left(L_1^*\right) = K_2^*\left(L_2^*\right) \tag{6.12}$$

provided

$$q_0^* = \frac{\left(1-\dfrac{k_1}{k_2}\right)\left(1+\dfrac{k_1}{k_2}-\dfrac{2k_1}{k_2}\,\dfrac{\alpha_1}{\alpha_2}\,\dfrac{\left(\lambda_2+2\mu_2\right)}{\left(\lambda_1+2\mu_1\right)}\right)}{\left(1-\dfrac{k_1}{k_2}\,\dfrac{\alpha_1}{\alpha_2}\,\dfrac{\left(\lambda_2+2\mu_2\right)}{\left(\lambda_1+2\mu_1\right)}\right)^2} \tag{6.13}$$

and

$$\frac{k_1}{k_2}\,\frac{\alpha_1}{\alpha_2}\,\frac{\left(\lambda_2+2\mu_2\right)}{\left(\lambda_1+2\mu_1\right)} \ne 1\ . \tag{6.14}$$

When

$$\frac{\alpha_1}{\alpha_2}\,\frac{\left(\lambda_2+2\mu_2\right)}{\left(\lambda_1+2\mu_1\right)} = \frac{k_2}{k_1} \tag{6.15}$$

then (6.12) is satisfied for all $0 \le q_0^* \le 1$ provided $k_1 = k_2$.

From (6.11) and (6.13),

$$K_1^*(0) = \frac{k_1}{k_2}\left[F^2\left(q_0^*\right) - G\left(q_0^*\right)\right]^{\frac{1}{2}} \tag{6.16}$$

and

$$P_{\text{in}}^* - P_{\text{out}}^* = 1 - \left[F^2\left(q_0^*\right) - G\left(q_0^*\right)\right]^{\frac{1}{2}} \tag{6.17}$$

where

$$F\left(q_0^*\right) = 1 - \frac{\alpha_1}{\alpha_2}\,\frac{\left(\lambda_2+2\mu_2\right)}{\left(\lambda_1+2\mu_1\right)} + \frac{\alpha_1}{\alpha_2}\,\frac{\left(\lambda_2+2\mu_2\right)}{\left(\lambda_1+2\mu_1\right)}\left(1-q_0^*\right)^{\frac{1}{2}}\ , \tag{6.18}$$

$$G\left(q_0^*\right) = \frac{\alpha_1}{\alpha_2}\,\frac{\left(\lambda_2+2\mu_2\right)}{\left(\lambda_1+2\mu_1\right)}\,\frac{k_2}{k_1}\,q_0^*\,\frac{L_1^*}{\left(1-L_1^*\right)} \tag{6.19}$$

and

$$F(0) = 1\ , \qquad G(0) = 0\ . \tag{6.20}$$

From (6.20) and (6.17),

$$P_{\rm in}^* - P_{\rm out}^* = 1 - \frac{k_2}{k_1}\, K_1^*\,(0)\,. \tag{6.21}$$

The pressure difference $P_{\rm in}^* - P_{\rm out}^*$ and the permeability $K_1^*(0)$ which are related through (6.21) are important scaled quantities in the understanding of the working of the double mask and are fully analised in terms of the functions $F^2\big(q_0^*\big)$ and $G\big(q_0^*\big)$ in Section 8.

6.2 Parameter reduction

The dimensionless parameters involved are the zero flow permeability ratio $\frac{k_1}{k_2}$, the 'compressibility' ratio $\frac{\alpha_1}{\alpha_2}$, the elastic modulus ratio $\frac{\lambda_1+2\mu_1}{\lambda_2+2\mu_2}$ and the filter thickness ratio $L_1^*/(1-L_1^*)$. However an examination of the results in Section 6.1 indicates that the compressibility and elastic parameters only occur in combination leaving just three dimensionless groups:

$$\Lambda_{21} = \frac{(\lambda_2+2\mu_2)/\alpha_2}{(\lambda_1+2\mu_1)/\alpha_1}, \quad k_{21} = \frac{k_2}{k_1}, \quad L_{12}^* = \frac{L_1^*}{1-L_1^*}. \tag{6.22}$$

The implication of this observation is that a changed flow behaviour can be achieved by either adjusting the permeability parameters α_i or by adjusting the elastic parameters $\lambda_i + 2\mu_i$. In terms of this new set of parameters the expressions for the scaled permeabilities are given by:

$$K_1^*(x^*) \equiv \frac{K_1(x^*)}{k_2} = \frac{1}{k_{21}}\sqrt{F^2(q_0^*) - G^*(q_0^*, x^*)},$$

$$K_2^*(x^*) \equiv \frac{K_2(x^*)}{k_2} = \sqrt{1 - q_0^*(\frac{1-x^*}{1-L_1^*})}\,. \tag{6.23}$$

with

$$G(q_0^*, x^*) = k_{21}\Lambda_{21}\, q_0^* L_{12}^*(x^*)\,, \quad L_{12}^*(x^*) = \left(\frac{L_1^* - x^*}{1-L_1^*}\right)\,. \tag{6.24}$$

The scaled pressure difference is given by

$$\Delta P^* = P_{in}^* - P_{out}^* = 1 - \left[F^2(q_0^*) - G(q_0^*, 0)\right]^{\frac{1}{2}} \tag{6.25}$$

with

$$G(q_0^*, 0) = G(q_0^*) = k_{21}\,\Lambda_{21}\, q_0^*\, L_{12}^*\,, \quad F(q_0^*) = 1 - \Lambda_{21}\left(1 - \left(1 - q_0^*\right)^{\frac{1}{2}}\right)\,. \tag{6.26}$$

It is useful to think of the above results as determining the pressure drop required to drive a prescribed flow q_0^* through the two masks under steady state conditions. We will confine our attention to situations in which the pressure drop $\Delta P^* > 0$.

7 Double mask with constant permeabilities

Before we analyse the results for a double compressible mask we will present the solution for a double mask with constant permeabilities. This will make clearer the special properties of a double compressible mask.

It is easier to solve the problem of two masks with constant permeability directly than to take the limit of two compressible masks. The governing equations are (3.3), (3.4) with $K_n = k_n =$ constant and (3.8) subject to the boundary conditions (3.9), (3.10) and (3.11) and to the matching conditions (3.12), (3.13) and (3.14). Since the permeability is constant for each mask we solve for the displacements $u_1(x)$ and $u_2(x)$.

For Mask 1,

$$K_1 = k_1 \ , \tag{7.1}$$

$$u_1(x) = -\frac{q_0\,\eta}{2k_1\big(\lambda_1 + 2\mu_1\big)}\ x\ \left[2\left(L_1 + \frac{k_1}{k_2}\ L_2\right) - x\right]\ , \tag{7.2}$$

$$P_1(x) = P_{\text{in}} - \frac{q_0\,\eta\,L_2}{k_2}\left[1 + \frac{k_2}{k_1}\ \frac{(L_1 - x)}{L_2}\right]\ , \tag{7.3}$$

where $0 \le x \le L_1$. For Mask 2

$$K_2 = k_2 \ , \tag{7.4}$$

$$u_2(x) = u_1(L_1) - \frac{q_0\,\eta}{2k_2\big(\lambda_2 + 2\mu_2\big)}\ (x - L_1)(L_1 + 2L_2 - x)\ , \tag{7.5}$$

$$P_2(x) = P_{\text{in}} - \frac{q_0\,\eta}{k_2}\ (L - x)\ , \tag{7.6}$$

where $L_1 \le x \le L$ and

$$u_1(L_1) = -\frac{q_0\,\eta\,L_1}{2k_1\big(\lambda_1 + 2\mu_1\big)}\ \left(L_1 + \frac{2k_1}{k_2}\ L_2\right) < 0\ . \tag{7.7}$$

Also the pressure difference satisfies

$$P_{\text{in}} - P_{\text{out}} = \frac{q_0\,\eta\,L_2}{k_2}\ \left[1 + \frac{k_2}{k_1}\ \frac{L_1}{L_2}\right]\ , \tag{7.8}$$

which is also the relation between P_{out} and q_0.

Although the permeability is constant, the masks can deform and we see that for the displacement, $u_1(x) < 0$ for $0 \le x \le L_1$ and $u_2(x) < 0$ for $L_1 \le x \le L$.

Both $P_1(x)$ and $P_2(x)$ are increasing functions of x and the pressures match at the interface $x = L_1$. The pressure $P_2(x) \ge 0$ for all $L_1 \le x \le L$ provided

$$q_0 \le \frac{P_{\text{in}}\,k_2}{\eta\,L_2} \tag{7.9}$$

while $P_1(x) \geq 0$ for all $0 \leq x \leq L_1$ provided

$$q_0 \leq \frac{P_{\text{in}}\, k_2}{\eta\, L_2\, \left(1 + \frac{k_2}{k_1}\, \frac{L_1}{L_2}\right)}\,. \tag{7.10}$$

Equation (7.10) follows directly from (7.8) and is the condition for $P_{\text{out}} \geq 0$. Unlike the maximum fluid flux q_s given by (6.1) for the permeability $K_2(x)$ of the double compressible mask to be real, the flux (7.10) is independent of the effective Lamé constants, $\lambda_2 + 2\mu_2$, and depends on the pressure P_{in}.

We will not introduce scaled variables because we are focusing on compressibility effects on the permeability and they are absent in the double mask with constant permeabilities.

8 Results for a compressible double mask

In a double mask with constant permeabilities the pressure drop required to drive flux q_0 through the mask is given by (7.8),

$$P_{\text{in}} - P_{\text{out}} = q_0\, \eta \left[\frac{L_2}{k_2} + \frac{L_1}{k_1}\right]; \tag{8.1}$$

we have two resistances in series determining the through-flow. The pressure is continuous but the permeability is discontinuous across the interface between the filters. The through-flux increases in direct proportion to the applied pressure drop. Note especially that there is no upper bound on the through-flux; we will see that for compressible masks there is an upper bound.

For compressible filters there are two primary dimensionless parameters governing the flow behaviour: the zero flux permeability ratio k_{21}, and the poroelastic ratio parameter Λ_{21}. In the covid mask context it is sensible to have $k_{21} \geq 1$ so that larger particles are filtered out by the filter closest to the face; we will assume this is the case for the simulations. Before undertaking an analysis of the general situation it is useful to plot out some steady state solutions corresponding to fixed values of the zero flux permeability ratio k_{21}.

8.1 Preliminary simulations

8.1.1 The $k_{21} = 1, \Lambda_{21} = 1$ case

Note that this case includes the case in which both filters are identical, which we will refer to as the single filter case, but also includes cases with different values of α but compensating values of $\lambda + 2\mu$ arranged so that the poroelastic parameter ratio Λ_{21} remains unchanged; this feature may be significant in terms of mask design.

Plots of permeability through the mask (two filters) are displayed in Figure 2. We note that for zero flux conditions compressibility effects disappear and the scaled permeability $K^*(x) = 1$, as required by the scaling. As influx q_0^* levels increase from

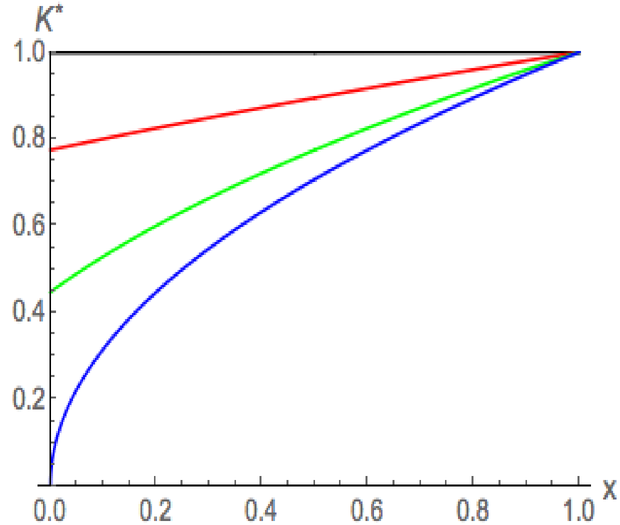

Figure 2: The $k_{21} = 1, \Lambda_{21} = 1$ single mask case: Local permeability variations $K^*(x)$ through the mask for increasing through-flux levels: $q_0^* = 0$ (top, black), then 0.2 (red), 0.4 (green), 0.5 (lowest, blue). The maximum possible (scaled) flux through the mask is $q_0^* = 0.5$ corresponding to the blue curve.

zero the permeability decreases uniformly according to our poroelastic model under the mask compression circumstances

$$\Delta P^* = P_{\text{in}}^* - P_{\text{out}}^* > 0 \tag{8.2}$$

of interest here.

This particular parameter set is special in that the (local) permeability is continuous through the mask; for all other parameter combinations there is a discontinuity across the interface $x^* = L_1^*$ between the two filters. The reader will recall that the external face of the mask ($x = 0$) is rigidly constrained by a porous grid, so that the compression is greatest here and thus the permeability $K^*(x)$ reaches a minimum at $x^* = 0$ and increases with distance from this outer mask face, as seen in Figure 2.

Of course no steady state solution is possible if the permeability is zero anywhere within the mask, and the first location to realise such a zero flux state is the external face of the mask $x^* = 0$. Once this happens the flow 'shuts down', so that there is an abrupt change in through-flux from a maximum value (of $q_0^* = 0.5$ for our present set of parameters as seen in Figure 2), to zero. Higher steady state flux levels than this maximum value are not possible basically because the pores in filter 1 have closed. Of course a higher pressure drop than $\Delta P^* = 1$ can be applied to the mask but the excess pressure will simply be taken elastically by the filter fibres[3].

The mask consisting of the two filters can be thought of as an equivalent single mask with effective global (or bulk) permeability defined by pressure drop across the

[3]It seems likely that non-linear effects will enter the picture near shut down, so our poroelastic model will fail, but none-the-less the general picture of virtually no through-flow (or pulsating flow) should be correct.

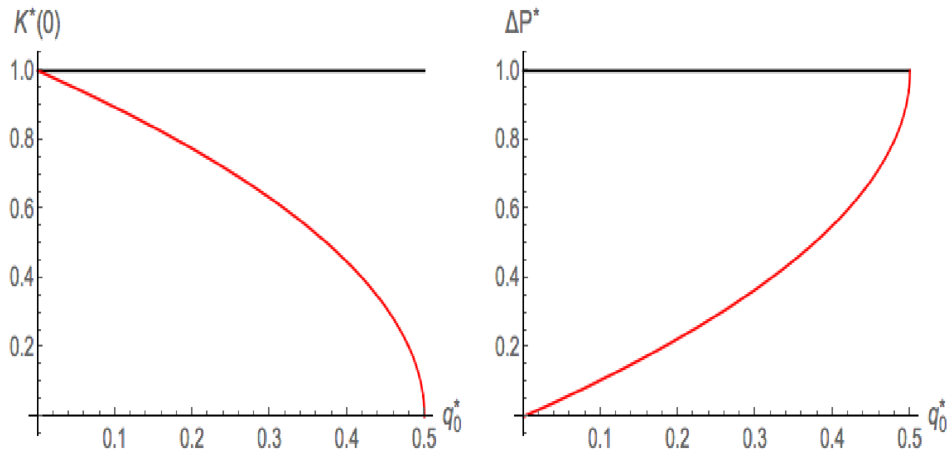

Figure 3: The $k_{21} = 1, \Lambda_{21} = 1$ single mask case: *Left*: Global permeability vs flux results: Note that zero global permeability occurs with a maximum through-flux of $q_0^* = 0.5$ *Right*: Pressure drop vs flux results: Note that the maximum pressure drop $\Delta P^* = 1$ occurs when the through-flux is maximal at $q_0^* = 0.5$.

two filters verses through-flux relation, which is determined by $K^*(0)$, see (6.21). This effective global permeability will be dependent on the through-flux and will vary from $K^*(0) = 1$ when $q_0^* = 0$, to $K^*(0) = 0$ when $q_0^* = 0.5$, see Figure 3 *Left*. The associated pressure drop verses flux relation is shown in Figure 3 *Right*; the maximal pressure drop ($\Delta P^* = 1$) is realised with a through-flux of $q_0^* = 0.5$. It should be noted that a mask consisting of a single filter (just filter 2) would allow the maximal through-flux $q_0^* = 1$[4].

8.1.2 The $k_{21} = 1, \lambda_{21} \neq 1$ case

Note the abrupt drop in the (local) permeability $K^*(x)$ across the interface between the two layers in the case when $\lambda_{21} = 2$, see Figure 4: *Left*. Flux shut down now occurs at a lower maximum flux level compared with the $\Lambda_{21} = 1$ case, of $q_0^* = 0.26 < 0.5$ due to the increase in the poroelastic ratio. The associated pressure drop vs flux relationship is shown in Figure 4 *Right*. Again shut down is abrupt; flux levels reduce to zero if the pressure drop exceeds the maximal value $\Delta P^* = 1$.

The effect of varying the poroelastic parameter ratio Λ_{21} (with $k_{21} = 1$) on the permeability and pressure drop is shown in Figure 5. There are two distinctly different cases:

1. Either curves hit the maximal flux value of $q^* = 1$ barrier. This occurs for smaller poroelastic ratio situations (Λ_{21}=0.1 (red), 0.2 (green)). Note that $q^* = 1$ corresponds to an un-scaled flux value of

$$q_s = \frac{k_2\big(\lambda_2 + 2\mu_2\big)}{2\alpha_2\,\eta\,L_2}\ ;$$

it is mask 2 (the inner mask) that controls the limiting behaviour.

[4]The thickness of the single layer mask being half that of the double mask.

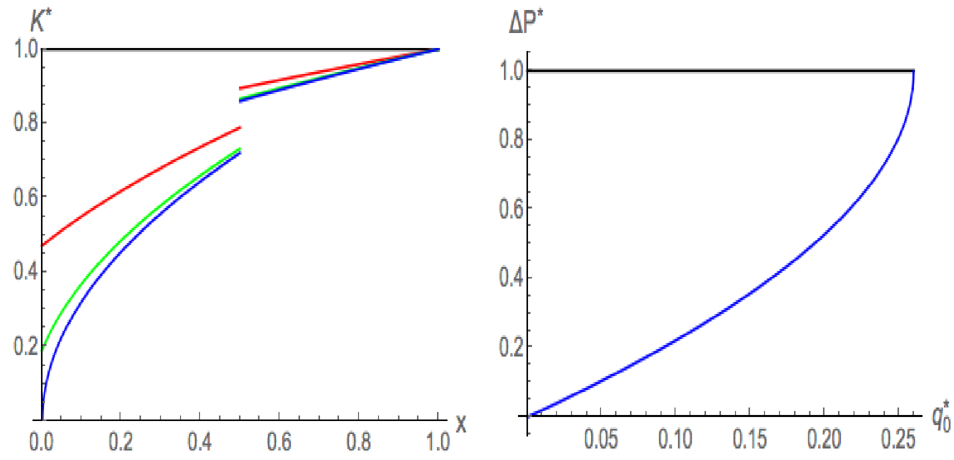

Figure 4: The $k_{21} = 1, \Lambda_{21} = 2$ case: *Left*: Local permeability variations through the mask for increasing through-flux levels: $q_0^* = 0$ top (black) curve, then 0.2 (red), 0.25 (green), 0.26 (blue, lowest). A (scaled) maximum flux level of $q_0^* = 0.26$ is possible (blue curve). *Right*: The associated pressure drop vs flux relationship.

2. Or curves hit the maximal pressure drop barrier $\Delta P^* = 1$. This occurs for poroelastic values larger than $\Lambda_{21} = 0.38$. Note that this corresponds to a real (unscaled) pressure drop of $(\lambda_1 + 2\mu_1)/\alpha_1$; it is mask 1 (the outer mask) that controls the limiting behaviour.

The blue curve, corresponding to $\Lambda_{21} = 0.38$, separates the two cases.

8.1.3 The $k_{21} = 2$ case:

Qualitatively the results in the $k_{21} = 2$ case are similar to those obtained with $k_{21} = 1$. First we present the $\Lambda_{21} = 1$ case, see Figure 6. The maximum possible flux is $q_0^* = 0.335 < 1$ which results if a maximal pressure drop of $\Delta P^* = 1$ is applied.

The results for variable poroelastic ratios (λ_{21}) are displayed in Figure 7.

8.1.4 Maximal through-flux levels

We have seen that through flux levels are reduced by increases of either the zero flux permeability factor k_{21} or the poroelastic parameter Λ_{21}. This may be useful for design purposes, so the dependence of the maximum flux possible through the two masks as a function of the two parameters is of interest. We can obtain this by equation $K^*(0) = 0$ and solving for q_0^*. Exact (but complicated) results are obtained and are plotted in Figure 8. Note that reduced maximum flux levels occur for larger values of Λ_{21}. Evidently the same maximum flux result can be obtained for a prescribed k_{21} by adjusting Λ_{21} as seen in Figure 8

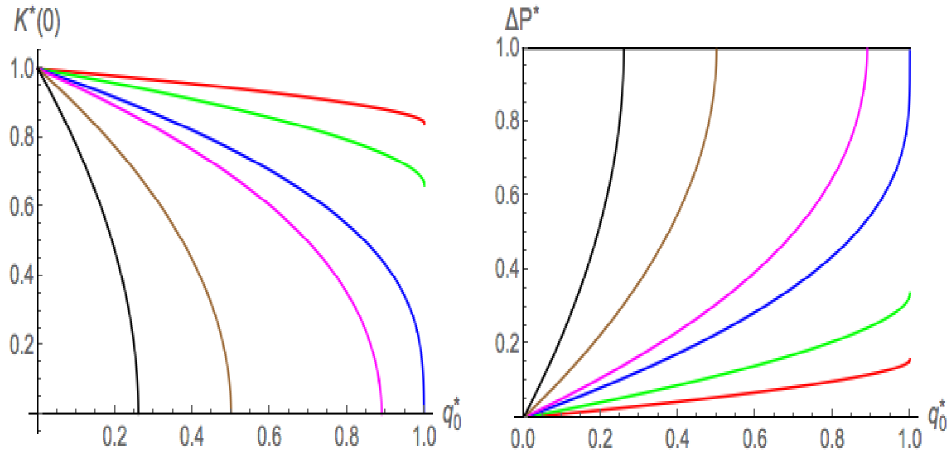

Figure 5: The $k_{21} = 1, \Lambda_{21}$ variable case: *Left*: Global permeability vs flux results for Λ_{21}= 0.1 (red), 0.2 (green), 0.38 (blue) $\cdots$ 2.0 (black). *Right*: The pressure drop vs. flux relationship for Λ_{21} = 0.1 (red), 0.2 (green), 0.38 (blue), $\cdots$ 2 (black). The blue curve with Λ_{21} = 0.38 separates out the two possible scenarios.

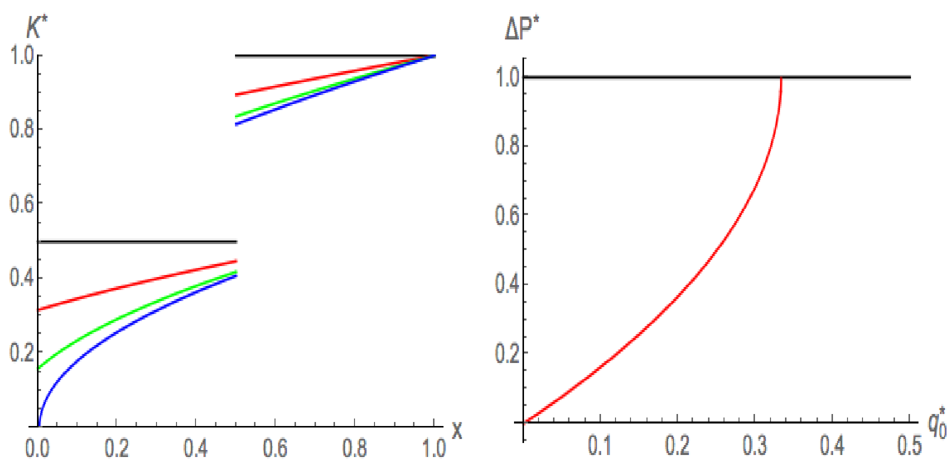

Figure 6: The $k_{21} = 2, \Lambda_{21} = 1$ case: *Left*: (Local) permeability variations through the mask for increasing through-flux levels varying from zero to cut-off (q_0^*=0 (black), 0.2 (red), 0.3 (green) , 0.335 (blue)). Cut off occurs at a flux level of $q_0^* = 0.334$ (the blue curve). *Right*: The pressure drop vs flux relationship.

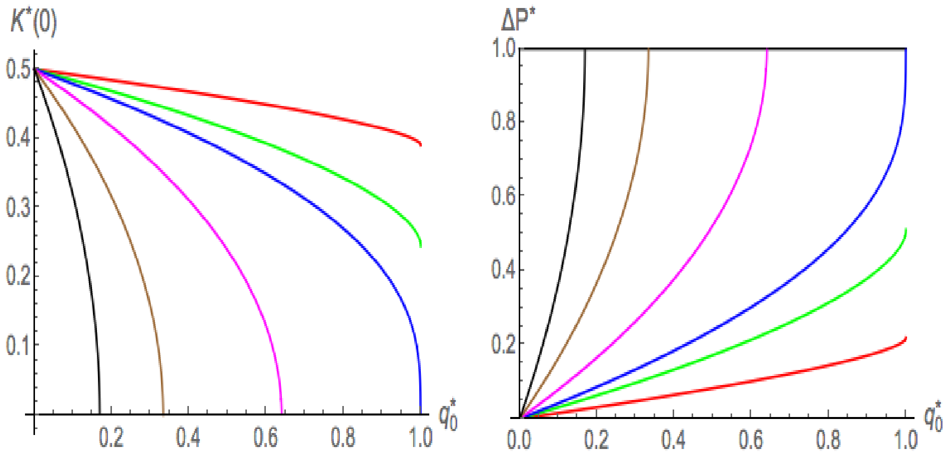

Figure 7: The $k_{21} = 2, \Lambda_{21}$ variable case: *Left*: Global permeability vs. flux results for Λ_{21}= 0.1 (red), 0.2 (green), 0.27 (blue), 0.5 (magenta), 1 (brown), 2 (black). *Right*: The pressure drop vs flux relationship for the same Λ_{21} range. The (blue) $\Lambda_{21} = 0.27$ case separates out the two possible scenarios.

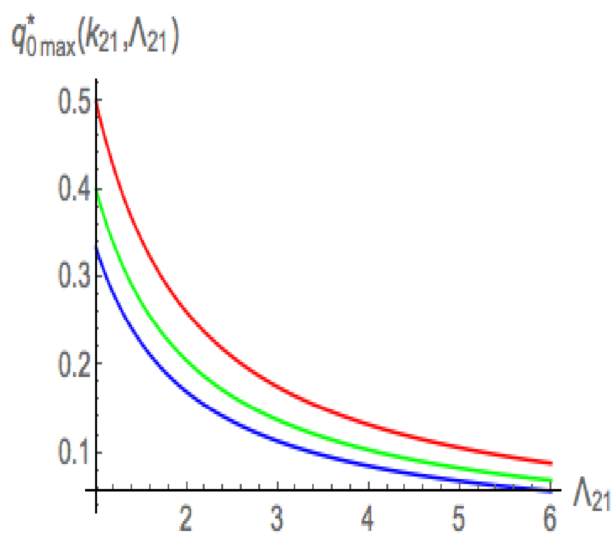

Figure 8: Maximal flux levels for two masks as a function of Λ_{21} for fixed values of $k_{21} = 1$ (red), $k_{21} = 1.5$ (green) and $k_{21} = 2$ (blue).

8.2 The general solution structure

As noted earlier real steady state solutions for mask flow exist in the range given by $q_0^* \leq 1$ and $\Delta P^* \leq 1$, otherwise the permeability goes to zero or becomes complex, indicating that no steady state flow is possible. In terms of the solution components (F^2, G) defined by (6.18) and (6.19) real values for pressure drop only exist if $F^2 \geq G$. When $F^2 = G$ the scaled pressure reaches its maximal value of $P^* = 1$, with a global permeability of $K_1^*(0) = 0$. With this in mind we plot in Figure 9 the functions $F^2(q_0^*)$ and $G(q_0^*)$ for a range of values of the poroelastic parameters k_{21} and Λ_{21}. Note that $G(q_0^*)$ is a linear function of q_0^* whereas $F^2(q_0^*)$ can either curve upwards or downwards depending on the values of the zero flux permeability ratio

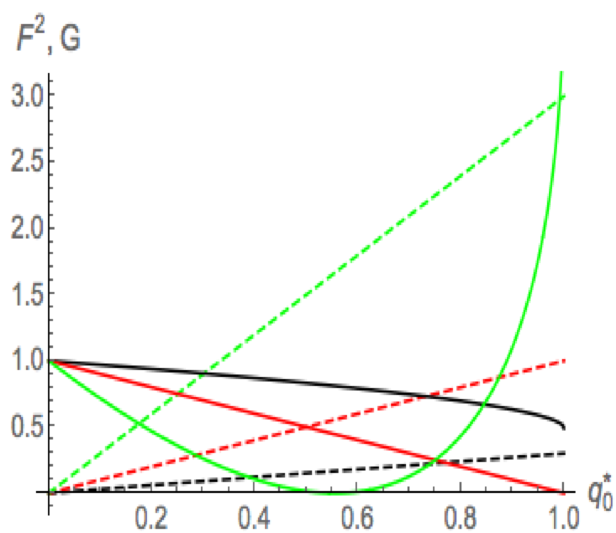

Figure 9: Plots for $F^2(q_0^*, k_{21}, \Lambda_{21})$ (solid curves), and $G(q_0^*, k_{21}, \Lambda_{21})$ (dashed curves) for $k_{21} = 1$, and $\Lambda_{21} = 0.3$ (black), 1 (red) and 3 (green). The curves for $\Lambda_{21} = 0.3$ (black) do not intersect. Those for $\Lambda_{21} = 1$ (red) intersect at one point. Those for $\Lambda_{21} = 3$ (green) the curves intersect at two points.

k_{21} and the poroelastic ratio Λ_{21}. This means that, over the allowable flux range $0 \leq q_0^* \leq 1$ there will be for $F^2(q_0^*) - G(q_0^*) = 0$ either: no solutions, one solution, or two solutions for q_0^*, depending on the poroelastic parameter values.

In Figure 9 we plot G and F^2 for a conductivity ratio $k_{21} = 1$, and a range of values of the poroelastic ratio Λ_{21}. For increasing values of Λ_{21} the F^2 and G curves first cross at $q_0^* = 1$ so that a transition between the different solution structures can be determined by equating $F^2(1)$ to $G(1)$. This gives the result that, if the thickness adjusted permeability ratio $k_{21}\frac{L_1^*}{1-L_1^*}$ is greater than the critical value

$$k_{21}^{crit}(\Lambda_{21}) = \frac{(1-\Lambda_{21})^2}{\Lambda_{21}}, \tag{8.3}$$

then there is just one solution for q_0^* (given by $q_0^* = 0.126$ in the $k_{21} = 1$ case). The critical k_{21} curve is plotted in Figure 10. Above this curve (the shaded region) there

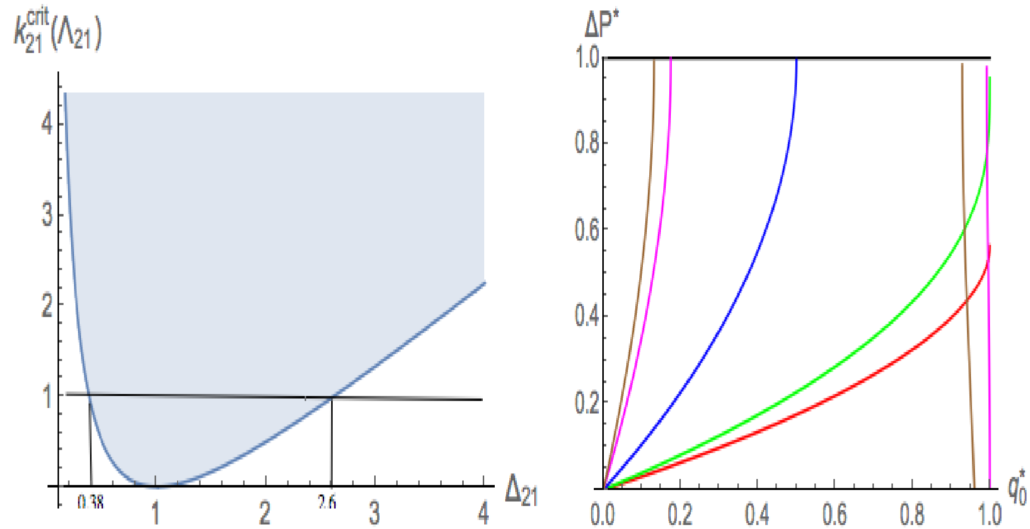

Figure 10: The critical k_{21} curve ($k_{21}^{crit}(\Lambda_{21})$) and solution branches in the $L_1^* = 1/2$ case: *Left*: The critical curve splits the parameter space into three regions (left, above and right). *Right*: Solution curves corresponding to $k_{21} = 1$. The red curve (with $\Lambda_{21} = 0.3$) is in the small lambda range, the blue curve ($\Lambda_{21} = 1$) is in the medium lambda range, with the green curve ($\Lambda_{21} = 0.38$) splitting the two solution zones. The (two) magenta curves correspond to ($\Lambda_{21} = 3$) are in the large lambda range.

is just one solution for q_0^*, to the left of this critical curve there are no solutions, while to the right there are two solutions. In the case in which $k_{21} = 1$ the regions are defined by: the small lambda range $(0, 0.38)$, the medium range $(0.38, 2.6)$, and the high lambda range > 2.6, see Figure 10 *Left*. The associated $\Delta P^*(q_0^*)$ solution curves are displayed in Figure 10 *Right*. In the small lambda range there is a single solution (the red curve) with flux levels increasing in response to the pressure drop ΔP^* until the maximum through-flux of $q_0^* = 1$ is reached (asymptotically) with $\Delta P^* < 1$; the maximum possible pressure drop is not reached. In the medium lambda range there is a single solution (shaded region blue curve) with flux levels increasing with the applied pressure drop until this reaches its maximal value $\Delta P^* = 1$, with a value of q_0^* less than its maximal value of unity. As described earlier, shut down occurs for higher pressure drops. This medium lambda range includes the $k_{21} = 1, \Lambda_{21} = 1$ single filter case. In the large lambda range ($\Lambda_{21} = 3$ (magenta) there are two solution branches.

Examples of solutions in the small and medium lambda range have been described before. All these solutions continuously evolve from an initial no flow $(\Delta P^*, q_0^*) = (0, 0)$ state. The small q_0^* branch in the large lambda case also evolves from an initial no flow state, but the second (large q_0^*) branch does not connect onto this zero flux state. In Figure 11 *Left* we have plotted pressure drop vs flux results in the $k_{21} = 1$ case with $\Lambda_{21} = 2.6$ and 3, 4 (the large lambda range). Note that $\Lambda_{21} = 2.6$ lies on the border of the large/medium parameter range and there is a single solution branch (the red curve) which matches the solutions in the neighbour-

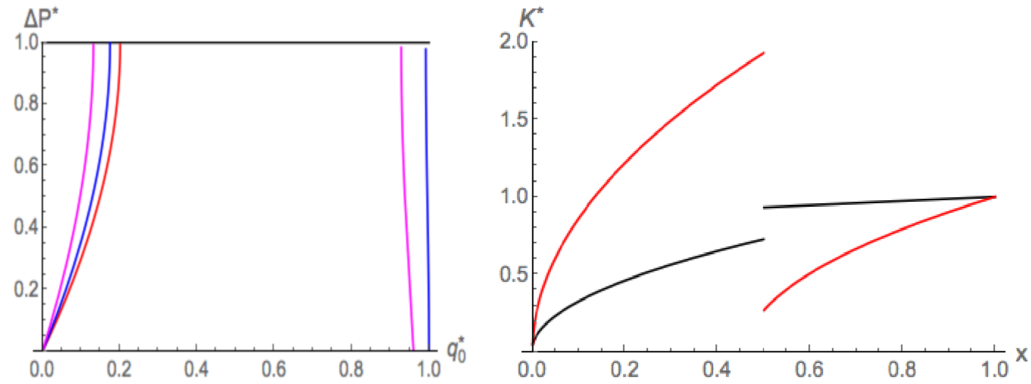

Figure 11: Two possible solutions in the large Λ_{21} case with $k_{21} = 1$: *Left*: $\Delta P^*(q_0^*)$. The red curve corresponds to $\Lambda_{21} = 2.6$ which lies on the critical curve so there is just one branch. The blue curve ($\Lambda_{21} = 3$) and magenta ($\Lambda_{21} = 4$) curves correspond to $\Lambda_{21} > 2.6$; there are two branches. *Right*: Local permeability variations through the mask for the two possible solution branches with $\Lambda_{21} = 4$. The black curve ($q_0^* = 0.126$) corresponds to the normal (small q_0^*) branch, the red curve ($q_0^* = 0.929$) to the large flux branch.

ing medium lambda parameter range. For larger values of Λ_{21} a second (large q_0^*) branch opens up (the blue curve), indicating that under steady state circumstances the same pressure drop can result in either a small or a large through-flux. Evidently the flow behaviour through the mask will be different in the two cases.

Figure 11 *Left* displays the pressure drop vs. flux relation for Λ_{21} values close to the transitional value of $\Lambda_{21} = 2.6$ (red curve). One can see the two branches (blue, magenta) opening up for $\Lambda_{21} = 3$ and 4; both branches move to the left as Λ_{21} increases.

To examine this second branch situation further we determine permeability variations through the mask for the two solutions corresponding to a pressure drop of $\Delta P^* = 0.951$ close to maximal pressure drop of unity. The corresponding flux levels are $q_0^* = 0.131$ and $q_0^* = 0.928$. The results for the (local) permeability variations through the masks are displayed in Figure 11 *Right*. In the (normal) small lambda branch case (the black curve) the variations in permeability within filter 2 are moderate with larger variations through the external filter 1, whereas in the large q_0^* branch there are large variations in permeability through both filters. As indicated earlier the small flux branch results from a (gradual) increase in pressure drop from zero, so this is indeed the situation one would normally expect. If, on the other hand, the pressure drop across the mask is at its maximal value of unity (and so is 'at' shut down) then the through-flux may either be at a maximal value or zero, and a small change in the applied pressure may cause the solution to switch branches.

In explanation the external pressure drop on the mask can be either taken up in filter 1 fibres or filter 2 fibres, and what happens depends on history. A slow build up in pressure forcing will likely result in the low flux solution whereas an abrupt pressure change will compress filter 2 before filter 1 responds, giving rise to the high flux result.

9 Conclusions

The objective of this work was to assess the benefits of using a mask with two filters, and we focused our attentions here on the steady-state flow-through behaviour under flow out conditions. Of particular interest was the effect of filter compressibility on the flow-through behaviour. The thought was that using two filters may make it possible to design a mask that is both comfortable under normal breathing conditions (allowing relatively free exchange of air) and yet relatively impermeable under high flux expulsion (sneezing) conditions. The results we obtained showed that the reduction in permeability required to produce this changed behaviour could be achieved using either a single filter compressible mask or by using two filters with different poroelastic parameters. However a more dramatic change in behaviour is possible using two filters, and the poroelastic parameters can be more easily adjusted.

An interesting feature of the two masks problem (as distinct from the single mask problem) is the presence of a second steady state solution which is not likely to be realised under normal conditions.

Future work will be to address the particle filtering issues.

References

[1] Parker K, Mehta R and Caro C. Steady flow in porous elastically deformable materials, J App Mech, **54** (1987), 794–800.

[2] Kory J, Krupp AU, Please CP and Griffiths IM. The effect of compressibility on the behaviour of filter media, IMA J App Math, 2020 doi:10.1093/imamat/.

[3] Howell P, Kozyreff G and Ockendon J. Applied Solid Mechanics, Cambridge University Press, Cambridge 2009, pp 408–412.